Swirl Coaxial Injector Element Characterization for Booster Engines

PRA - SA - ATC/2 NASA - MSFC 6 MAY 88

Gregory M. Meagher
Jeffrey A. Muss

Aerojet TechSystems Company
Sacramento, CA

ABSTRACT

Recent hot fire testing at the Marshall Space Flight Center (MSFC) has indicated the swirl-coaxial element to be a viable candidate for the STBE injector. Plans are to test the current 40K lbf thrust injector at the higher chamber pressure and colder fuel temperature which are anticipated for STBE. Aerojet TechSystems Company has conducted an in-house IR&D cold flow program to characterize the swirl coax element over a range of operating points. This paper presents these results and compares them to the hot fire data. Predictions for compatibility, performance and stability are then presented for the uprated test conditions.

INTRODUCTION

Recently NASA has conducted test programs at the Marshall Space Flight Center (MSFC) to develop a technology base for LOX/methane combustion devices applicable to high pressure booster engines (Reference 1). Concept studies have indicated methane offers performance, cost, availability, chamber cooling and environmental advantages when compared to the denser hydrocarbon fuels. One of the injectors tested by NASA/MSFC was designed and built by Aerojet TechSystems Company under contract NAS8-33205 (Reference 2).

The injector assembly consists of a post type manifold with a platelet coaxial swirler injector pattern. Nine tests were conducted with this hardware over a chamber pressure range of 1400 to 2300 psia and mixture ratio varying between 2.5 and 3.4. The fuel temperature varied between 70° and 88°F. Further tests are planned at higher chamber pressures, approximately 3000 psia, and colder methane temperature, down to -60°F.

Aerojet conducted an in-house program to identify any potential risks for future testing and to better understand the existing hot fire data. During this program, the hot-fire test data was evaluated to define the absolute performance, thermal, and stability trends associated with a swirl coaxial element injector. Cold flow experiments were conducted to measure drop size, mixing efficiency and spray cone angle trends with operating conditions. These data in conjunction with state-of-the-art models were used to predict test results for higher chamber pressure and/or lower fuel temperature.

SWIRL COAX INJECTOR

The tested injector produces approximately 40,000 lbf thrust and was designed to meet the requirements listed in Table I. The injector, shown in Figure 1, has 60 coaxial elements. A bonded platelet stack was placed at the entrance to the posts and provided a tangential vector to the LOX spray. The resulting swirl enhances the LOX atomization and intra-element mixing. The

TABLE I

INJECTOR DESIGN REQUIREMENTS

Chamber Pressure:	1750 to 3000 psia
Fuel:	Methane
Temperature	Ambient
Maximum Interface Pressure	3800 psia
Oxidizer:	Oxygen
Temperature	185°R
Maximum Interface Pressure	4200 psia
Propellant Mixture Ratio	3.5
Characteristic Velocity Efficiency	> 97%
Allowable Chamber Pressure Oscillations	$< \pm 5\% P_C$
Combustion Chamber:	
Throat Diameter	3.310 in.
Chamber Diameter	5.660 in.
Length (injector to throat	13.7
Contraction Ratio	2.92

injector face contains photoetched hydraulic circuits that provide face cooling and radial fuel injection in the element. An axial cavity configuration was included and sized for the first tangential frequency . Fuel is injected into the cavity from the face periphery to cool the cavity interface. Cooling also reduces the cavity depth by lowering the sound speed.

The swirl coaxial element was selected from several element configurations following combustion efficiency, combustion stability and thermal compatibility assessments. These analyses indicated the swirl element offered the least risk in achieving the 97% C* design requirement while still providing acceptable front end chamber wall temperature. The overall element diameter was .266 inch and included a .180 inch LOX past I.D. surrounded by a .023 inch fuel annulus gap.

COLD FLOW PROGRAM

Cold flow experimentation was conducted in Aerojet's Rocket Research and Development test zone's injector cold flow facility. Data obtained was used in defining hydraulic, stability, and performance characteristics. These data included element Cd, flow admittance, and pressure drop, drop size, drop distribution, spray angle, mixing and mass distribution.

Figure 2 shows a typical cold flow test setup. The element hydraulics were determined from flow and pressure measurements. Drop and spray data were obtained from spark shadowgraph

Figure 1. LOX/CH_4 Swirl Injector

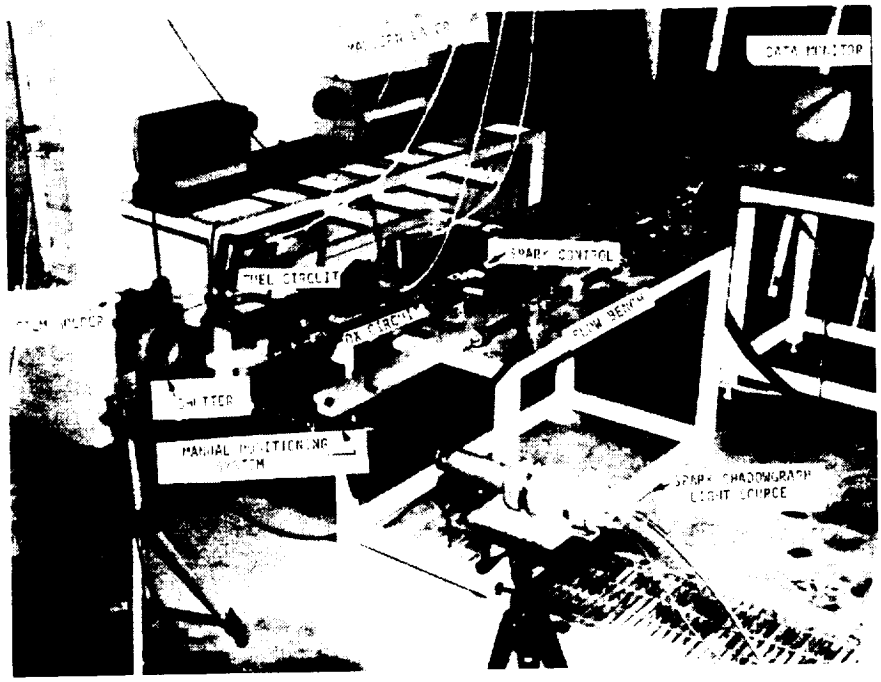

Figure 2. Aerojet's Cold Flow Facility

photos, strobe photos, and Malvern laser doppler system measurements. Mixing and mass distribution data were obtained by flowing the element over a collection device (referred to as a "milk-maid") which was segmented into 400 grids each 0.5 inch square. Each grid's flow was individually collected. Figure 3 shows the "milkmaid" test setup. Distribution and mixing data were generated by flowing two different fluids in the injector element fuel and oxidizer circuits and measuring their relative concentration or separate volume in the collector tube depending upon whether they were miscible or immiscible. Water was selected as the oxidizer simulant and aquaeous surcrose solution was the fuel simulant. The final concentration was measured by an automated refractometer. Test were also conducted using GN2 for the fuel simulant.

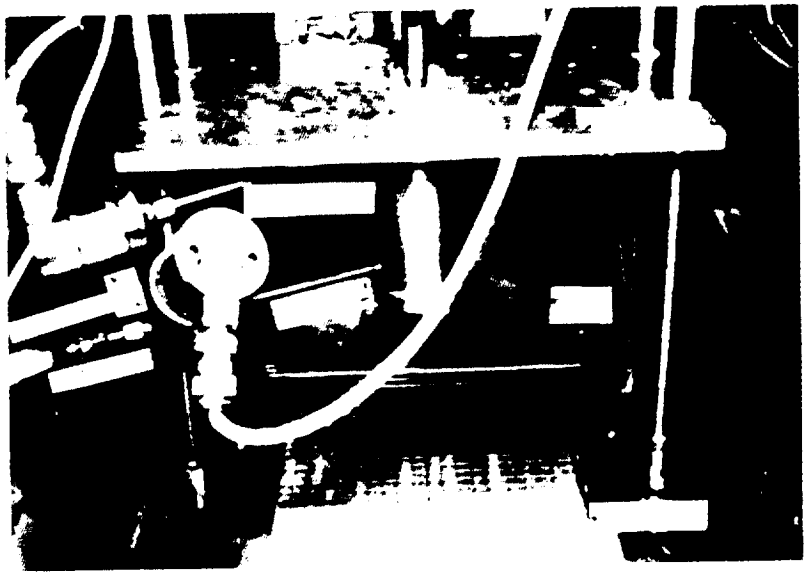

Figure 3. "Milkmaid" Test Setup

PERFORMANCE TRENDS AND PREDICTIONS

Table II is an expansion of the swirl injector test data presented in Reference 1. The requirement of a 97 percent minimum characteristic velocity efficiency was met for all test operating points. The characteristic velocity efficiency was found to improve with chamber pressure as shown in Figure 4. For a given chamber pressure the minimum efficiency occured at the mixture ratio corresponding to the peak theoretical charcteristic velocity. This trend is shown inFigure 5 and is indicative of mxing losses rather than incomplete vaporization. A Rupe mixing parameter, Em (Ref 3), was calculated to be approximately 0.86 for the hot fire data. This correlated very well with the mixing parameter value of 0.89 calculated for the cold flow tests having the same ratio of oxidizer to fuel momentum as the hot fire tests. Cold flow tests at momentum ratios corresponding with higher chamber pressure and/or colder fuel temperatures, indicate the mixing efficiency to remain essentially constant. Therefore the characteristic velocity efficiency is predicted to remain above 97 percent for the upcoming tests at MSFC.

INJECTOR CHAMBER COMPATIBILITY

Figure 6 shows the measured throat heat flux as a function of chamber pressure and mixture ratio. Also included is a heat flux prediction for the planned higher chamber pressure tests. The maximum heat flux is predicted to be 60 BTU/in^2 -sec which is still within the calorimeter chamber's capability.

Table II Injector Design Requirements

Test No.	t Sec	Pc psia	W_o lb/sec	P_{jo} psia	V_{oj} (ft/s)	W_f lb/sec	P_{jf} psia	V_{fj} (ft/s)	W_o/W_f	M	C* ft/sec	%C*	T_{ox} (°F)	T_f (°F)
3	8.2	1460	47.06	1710	141	18.85	1806	637	2.50	0.73	6155	97.8	-261	84.8
4	7.9	1686	57.44	2012	169	18.73	2016	608	3.07	1.12	6150	97.4	-268	88
5	8.0	1884	66.03	2284	134	19.23	2203	555	3.43	1.58	6140	98.5	-268	75
7A	4.3	2208	70.37	2677	206	27.80	2748	704	2.53	0.98	6250	99.1	-266	83.5
7B	7.9	2207	71.64	2689	206	27.02	2723	672	2.65	1.08	6216	98.1	-274	79
8	8.2	2244	74.81	2740	218	24.96	2695	625	3.00	1.38	6250	98.6	-268	74.8
9A	4.4	2274	78.42	2807	230	22.84	2669	566	3.43	1.84	6240	99.9	-266	76
9B	8.0	2302	79.16	2845	227	23.41	2704	562	3.38	1.80	6237	99.6	-275	71

$$\overline{M} = \frac{\dot{W}_{ox}\, V_{ox}}{\dot{W}_f\, V_f}, \qquad V_{ox} = \frac{144\ \dot{W}\ \text{Test}}{Cd_{ox}\, \rho_{ox}\, A_{ox}}, \qquad Cd_{ox} = \text{Cold Flow}, \qquad V_f = \frac{144\ \dot{W}\ \text{Test}}{\rho_f\, A_f\, Cd_f}, \qquad Cd_f = \frac{\dot{W}\ \text{Test}}{\dot{W}\ \text{1-D}}$$

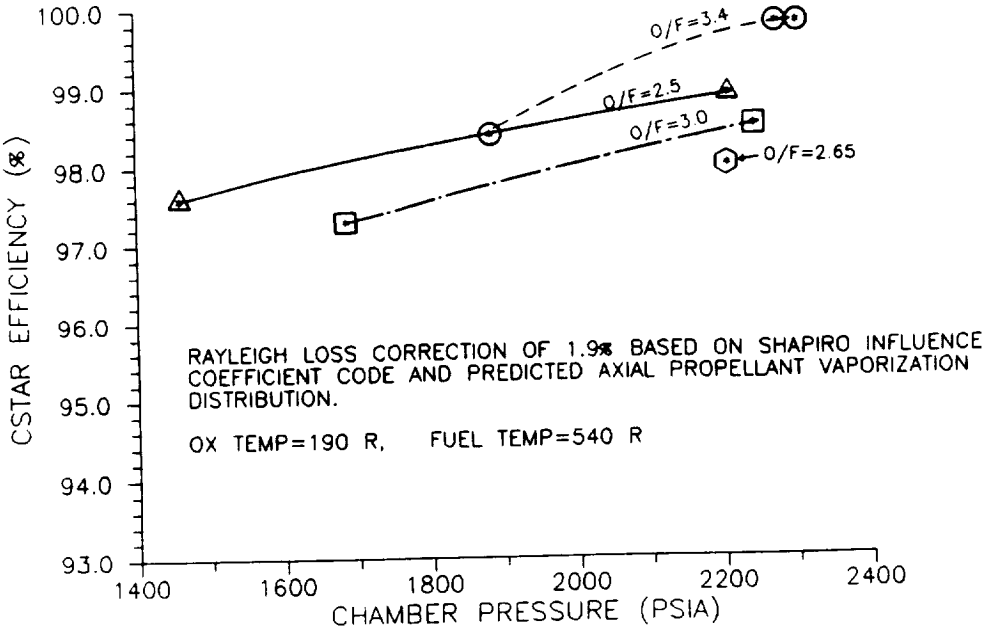

Figure 4. CSTAR Efficiency vs. Chamber Pressure

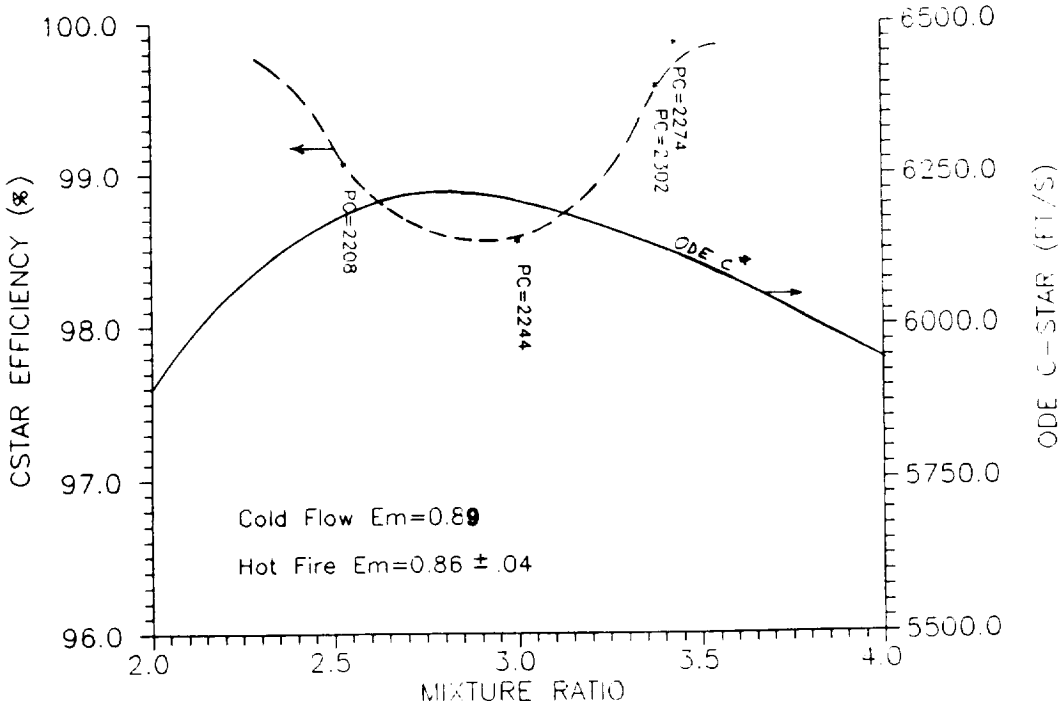

Figure 5. CSTAR Efficiency vs. Mixture Ratio

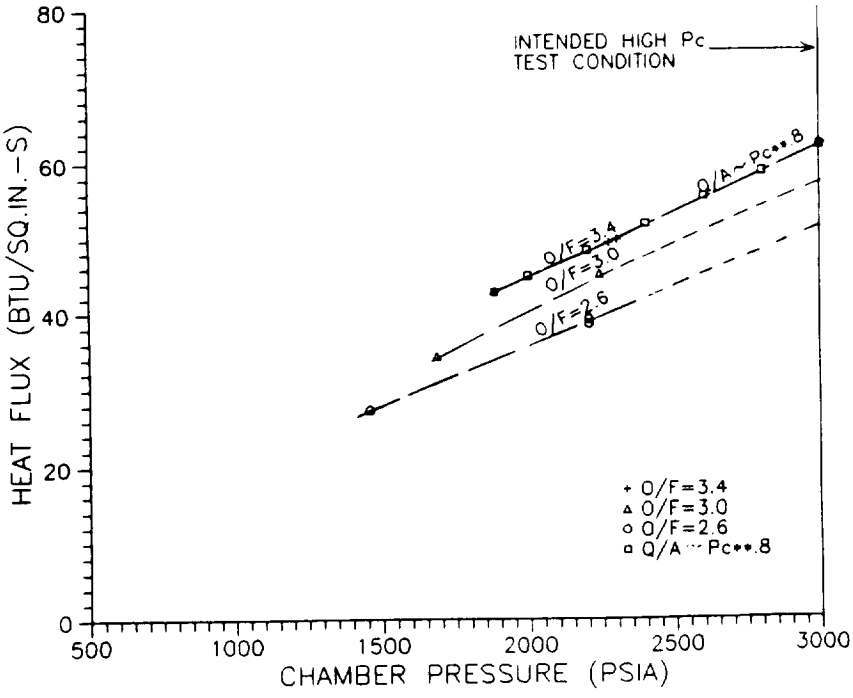

Figure 6. Heat Flux vs. Chamber Pressure

Chamber heat flux versus axial position as a function of chamber pressure and mixture ratio is shown in Figures 7 and 8 respectively. Also shown in Figure 7 is the LOX vaporization profile. As shown in these figures, the chamber barrel heat flux begins to decrease after approximately seven inches. This along with the vaporixation profile indicates that combustion has essentially been completed. These curves also show that no abnormal behavior occurred for the front end heat flux with changes in momentum ratio. Implied is that no significant spray fan effects occurs with changing operating conditions.

Cold flow testing verified that only small changes in spray fan angle (momentum angle) occur with changing momentum ratios. Figure 9 shows spray angle (momentum angle) as a function of momentum ratio as determined from spark shadowgraph and "milkmaid" data. The spray angle was measured directly from the spark shadowgraph and calculated using the mass distribution contour and element position during "milkmaid " testing. As momentum ratio increases, which corresponds to more oxidizer stream influence, the spray angle asymptotically approaches the cone angle for oxidizer flow only. Cold flow tests showed that for oxidizer flow only the angle remained constant with pressure. Figure 10 shows that small changes in element mass distribution occurred with changing momentum ratio. Also shown are the Em and spray angle values calculated.

Based on these data, any spray fan impingement on the chamber wall would move upstream approximately 0.5 inch for at the higher momentum ratios corresponding to the upcoming tests. Therefore good wall compatibility is predicted to still occur at the higher chamber pressures and colder fuel temperatures.

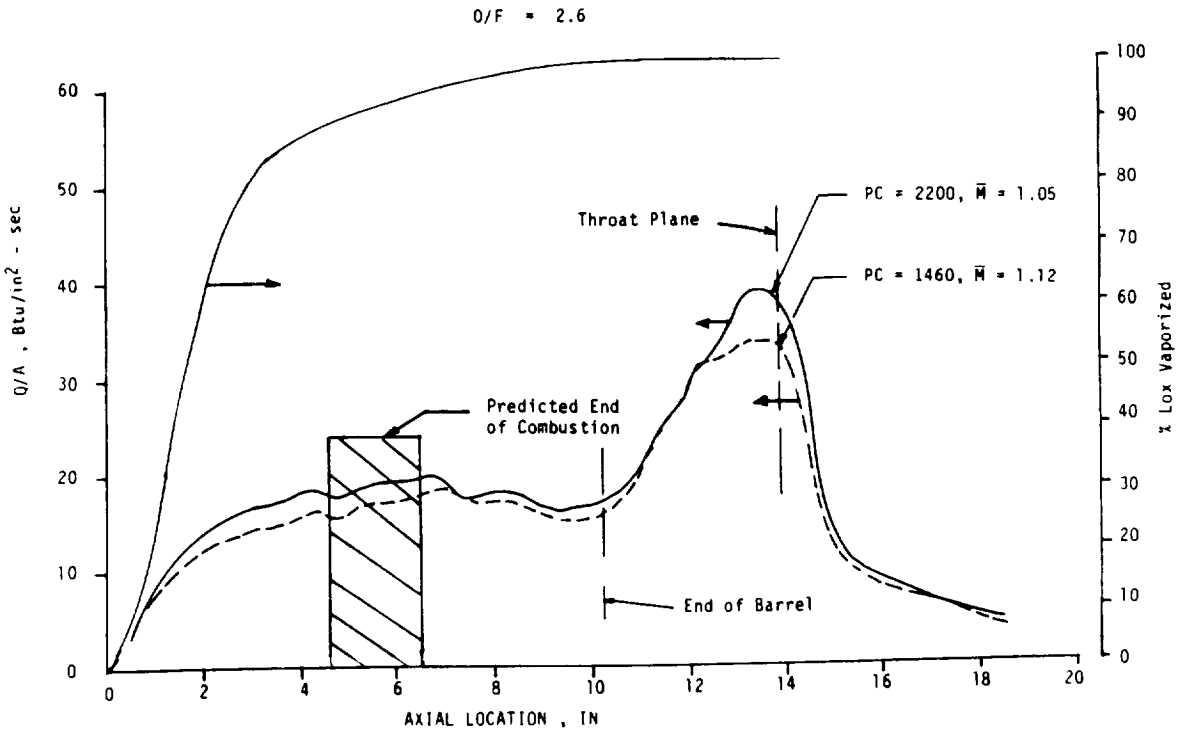

Figure 7. Heat Flux vs. Axial Position for Variable Chamber Pressure

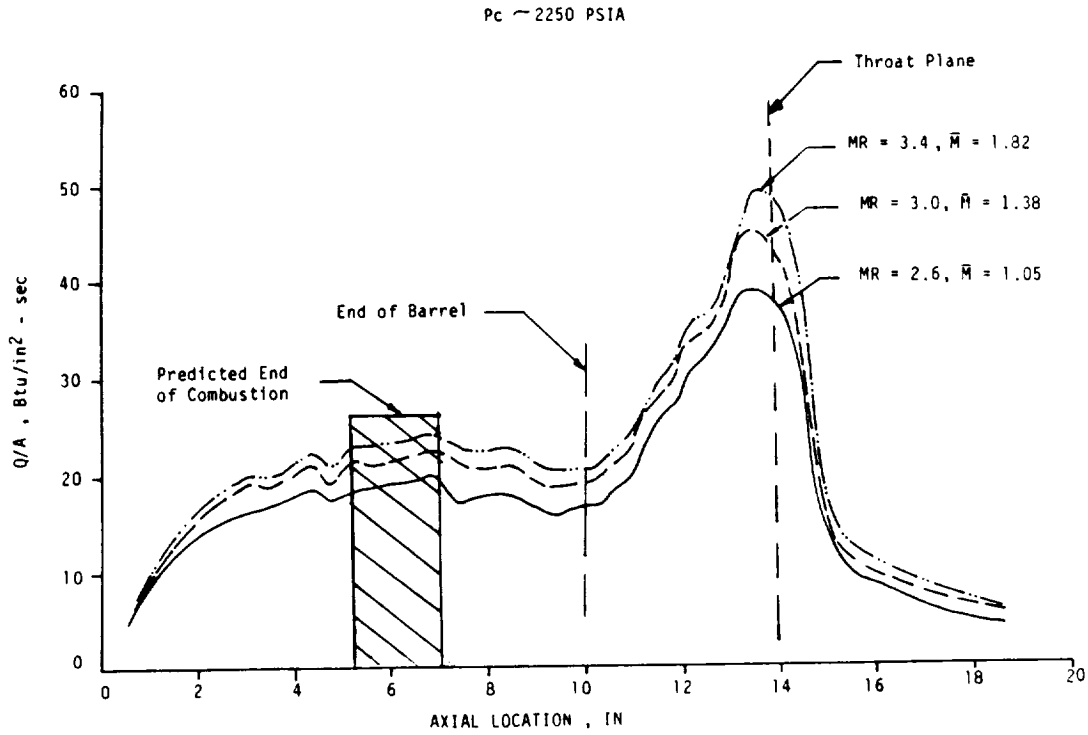

Figure 8. Heat Flux vs. Axial Position for Variable Mixture Ratio

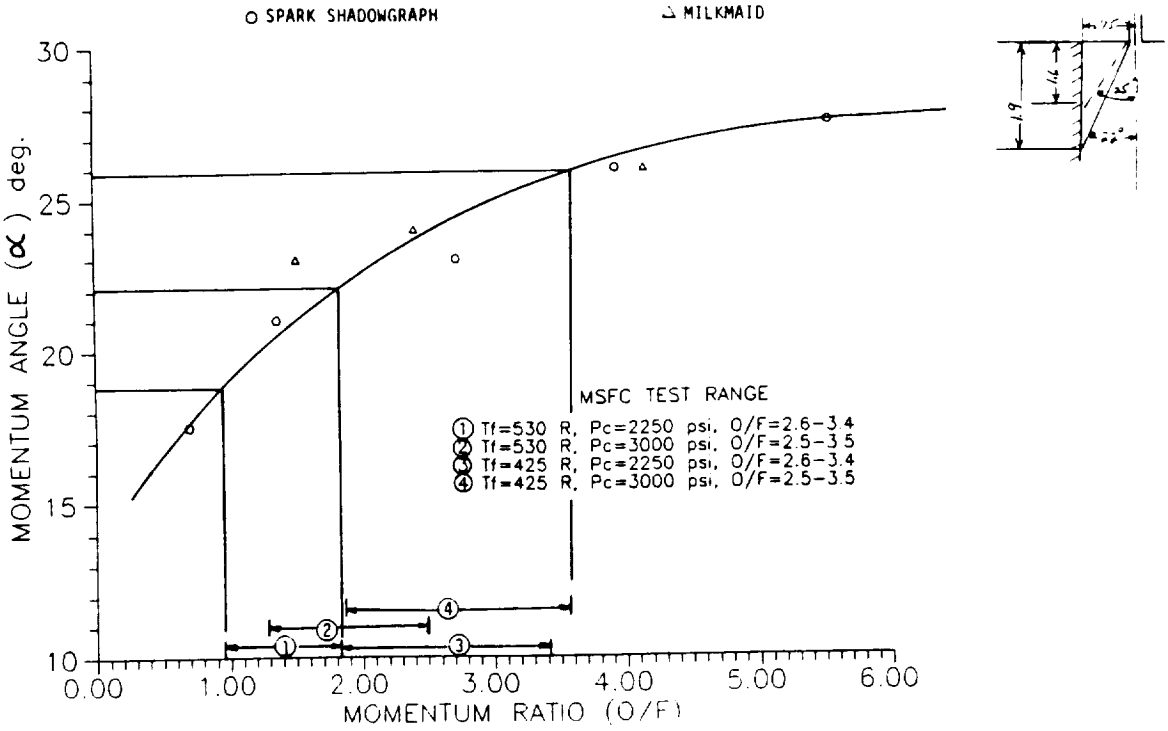

Figure 9. Spray Angle vs. Momentum Ratio

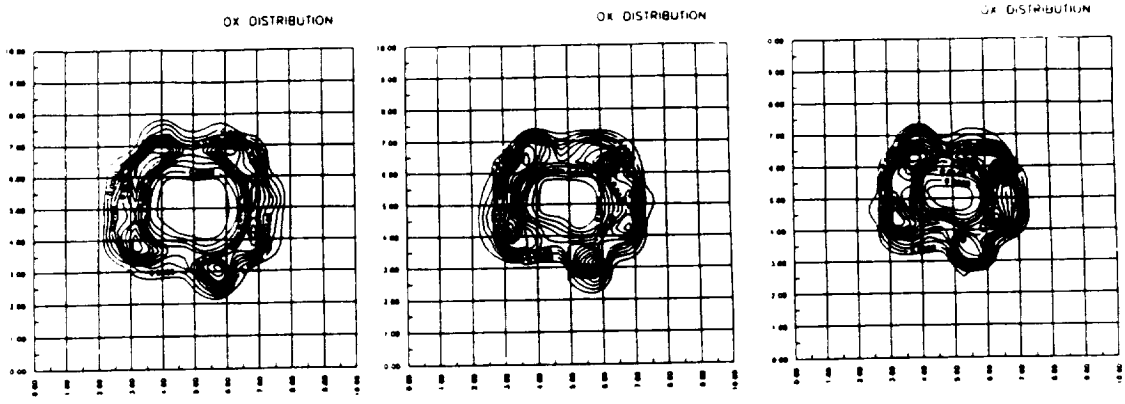

Figure 10. Mass Distribution as a Function of Momentum Ratio

COMBUSTION STABILITY

The observed combustion characteristics of the 40K injector were used to correlate sensitive inputs to the combustion stability models. These models were used to categorize observed instabilities, i.e., chug, burning coupled or injection coupled. The correlated models were then used to predict the expected stability behavior for increased chamber pressure and reduced fuel temperature testing.

The combustion stability data generated during initial testing was limited. Pressure oscillation amplitude and frequency were measured in the propellant fuel and oxidizer manifolds, and in some cases, accelerations were measured on LOX feed system components. Table III summarizes the existing stability data. In many cases, there is no correlation between observed oscillations in the fuel and oxidizer manifolds. It was noted that the amplitude of the oscillations in both propellant circuits decreases with increasing chamber pressure (Fig.11). In spite of the apparent combustion instabilities, there was neither signs of injector face or chamber melting nor an increase in heat transfer rate, both of which are characteristic of combustion instabilities at such high chamber pressures.

The model correlation began with the low frequency oscillations (390-420 hz) observed during the Level 1 step in tests 7-9. These frequencies were assumed to be associated with chug instabilities because they only occurred at the lowest chamber pressures, and the frequencies are well below the anticipated first longitudinal (1L) and first tangential (1T) acoustic resonant frequencies for an undamped chamber, 1800 and 5200 hz, respectively. The total timelags initially used in the analysis were based on the injection velocities, atomization length and drop size generated for each of the test conditions by our swirl coaxial atomization model. These timelags were used as inputs in our Low Frequency Combustion Stability model (LFCS), which predicted chug frequencies on the order of 290 hz and chug stability boundaries near 1800 and 1500 psia for mixture ratios of 1.97 and 2.49, respectively. It was found that by using 65 percent of the predicted total timelag (the atomization timelag being approximately 12 times larger than the vaporization timelag), that the model predictions not only matched the observed instability frequencies for tests 8S and 9S, but also a chug stability boundary which predicted tests 3-5 to be

Table III Swirl Coax Injector Stability Data

Test No.	Pc psia	O/F	Oxygen Manifold		Fuel Manifold		Acceleration Levels		
			Pressure Peak-Peak psi	Primary Freq. Hz	Pressure Peak-Peak psi	Primary Freq. Hz	Lox Dome g	Lox Valve g	Primary Lox Dome Freq. Hz
3	1460	2.50	461	7400	144	60			
				7200					
				4700					
4	1686	3.07	400	3200	179	3300			
5	1884	3.43	444	4500	101	Broad Band			
				6500					
7a	1300	—	650	400	148	Broad Band	794		
7b	2207	2.65	270	1800	92	Broad Band	718		
8a	1320	1.97	525	390	120	390	350	900-1400	
8b	2244	3.00	170	4300	40	Broad Band	350	660-925	8900
9a	1240	2.49	500	420	80	Broad Band	388	1500	
9b	2302	3.38	150	Broad Band	30	Broad Band	388	600-935	

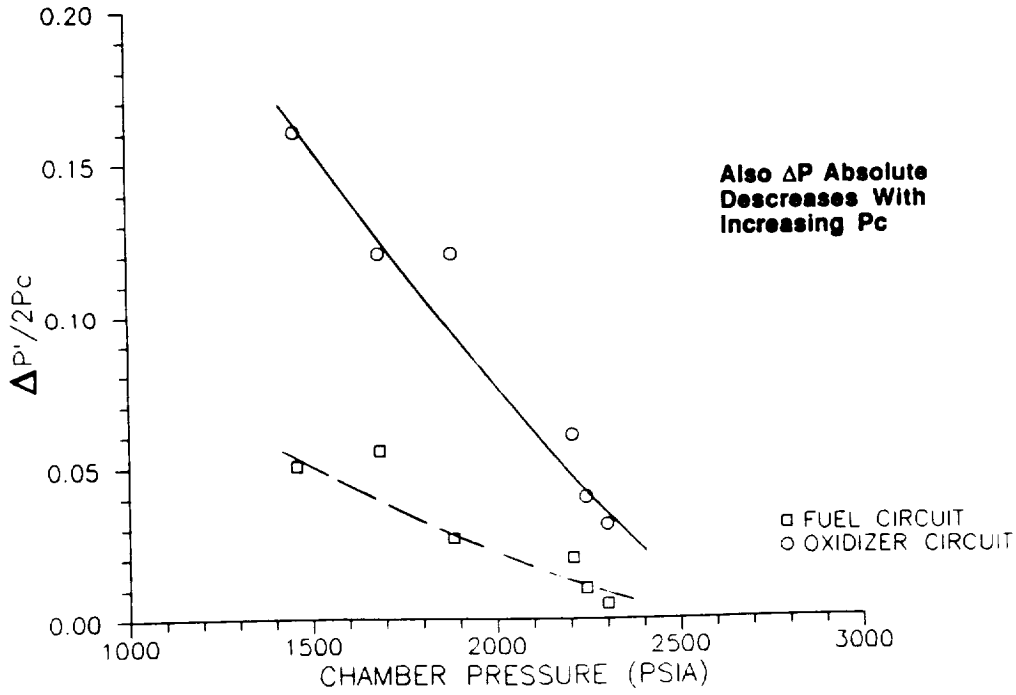

Figure 11. Manifold Pressure Perturbation vs. Chamber Pressure

chug stable, as observed (Figure 12). This analysis indicated that Level 1operation should be controlled to yield a mixture ratio of 3.0 and a chamber pressure greater than 1300 psia. The atomization model was then used to predict the timelags for operation with reduced methane temperature, and 65% of this value was used to predict the effect of reduce methane temperature on chug stability. Figure 13 indicates that reducing the fuel temperature from 530°R TO 425°R has a small impact on the chug stability boundary.

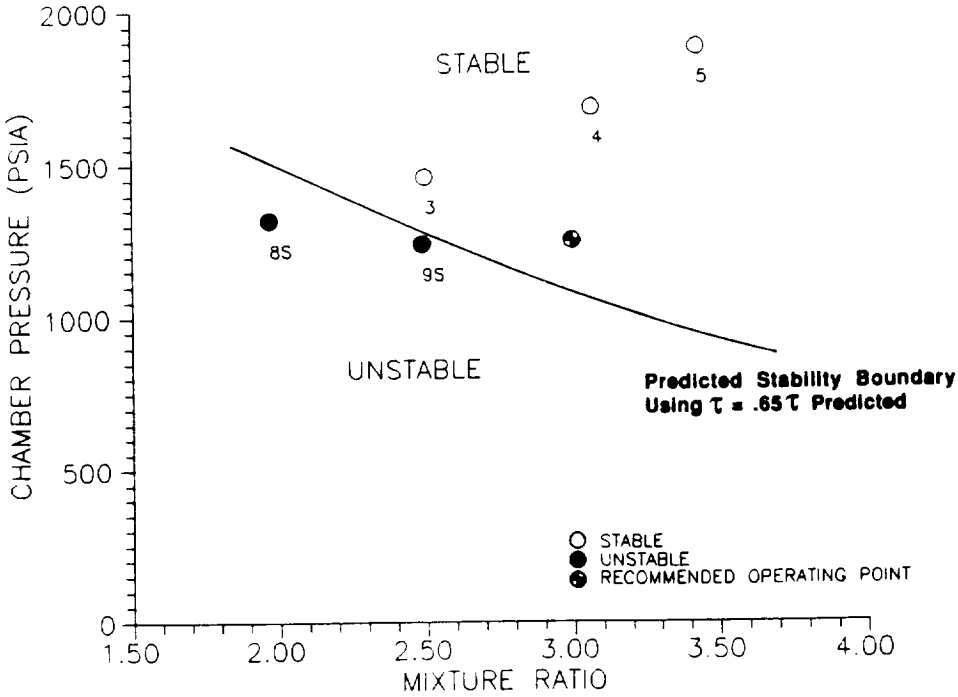

Figure 12. Chug Stability Limit

The oxygen drop size generated by the atomization model for the range of test conditions was on the order of 65 microns. This value agrees well with the data from the cold flow testing, as well as the measured performance and heat release profiles. The sensitive timelags associated with this drop size indicates that burning-coupled or intrinsec instabilities would couple with the chamber acoustics in the third tangential (3T) or first radial (1R) acoustic modes, which were predicted to occur between 10,000 and 12,000 hz. Since these frequencies are much higher than any of the observed oscillations, it was concluded that coupling does not occur in this manner. Atomization predictions made for the reduced fuel temperature operation indicated only a small change in oxygen drop size, and therefore very little change in sensitive timelag. Because the timelag only changes slightly, the reduced fuel temperature operation is not expected to affect intrinsic stability characteristics.

The injection-coupled stability behavior was analyzed using the High Frequency Stability model (HIFI) and the 65% of the total timelags generated by the analysis models. The model predicted that the 1L and 1T resonant acoustic frequencies were 1800 and 3300 hz,respectively. The 1T frequency is significantly lower than would be predicted with a simplified analysis due to depression of the resonant frequency by the acoustic cavity. Figure 14 shows the stability margin improves with increasing chamber pressure for both the 1L and the 1T modes at low mixture ratio (MR 2.5). This increase is due to a reduction in the total timelags as the fuel and oxygen velocities

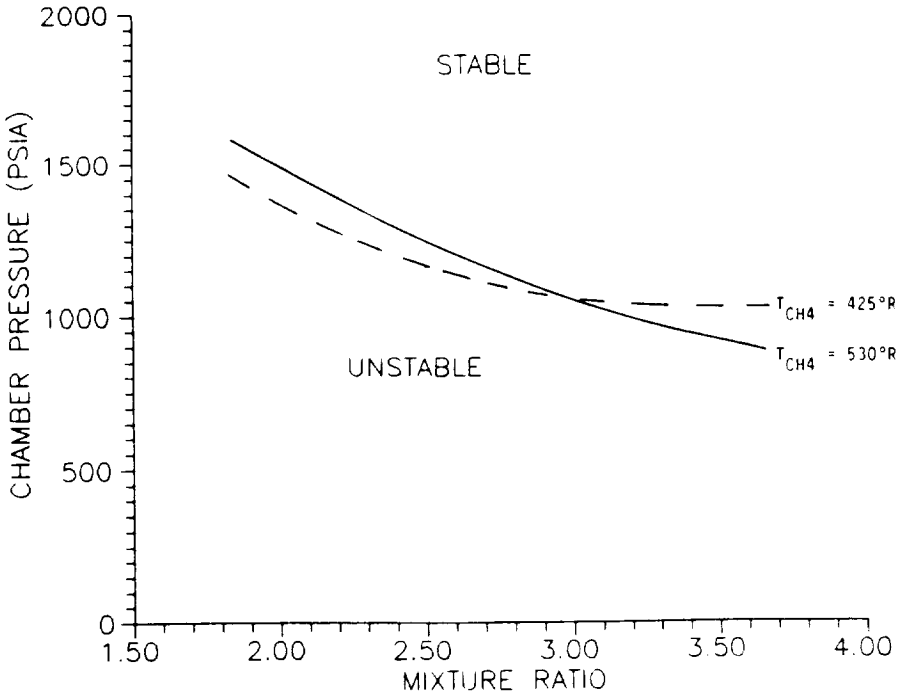

Figure 13. Chug Stability as a Function of Temperature

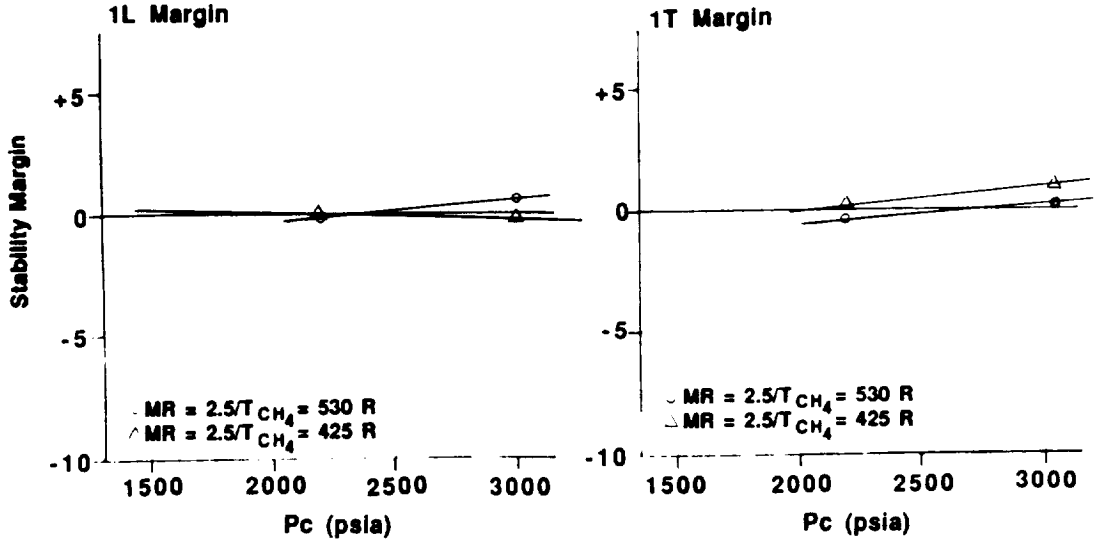

Figure 14. Stability Margin as a Function of Chamber Pressure for O/F = 2.5

increase,while the injector stiffness increases. Although the data is limited, the marginally unstable 1L behavior at 2200 psia corresponds well with the observed oscillation in Test 7B. The model also indicates that reducing the fuel temperature, and subsequently the injection velocity

and fuel circuit stiffness,is expected to have no adverse stability effects for the low mixture ratio operation. Figure 15 shows the predicted stability margin at the nominal mixture ratio (MR =3.5) for both ambient and reduced temperature fuel. The stability margin is predicted to improve with

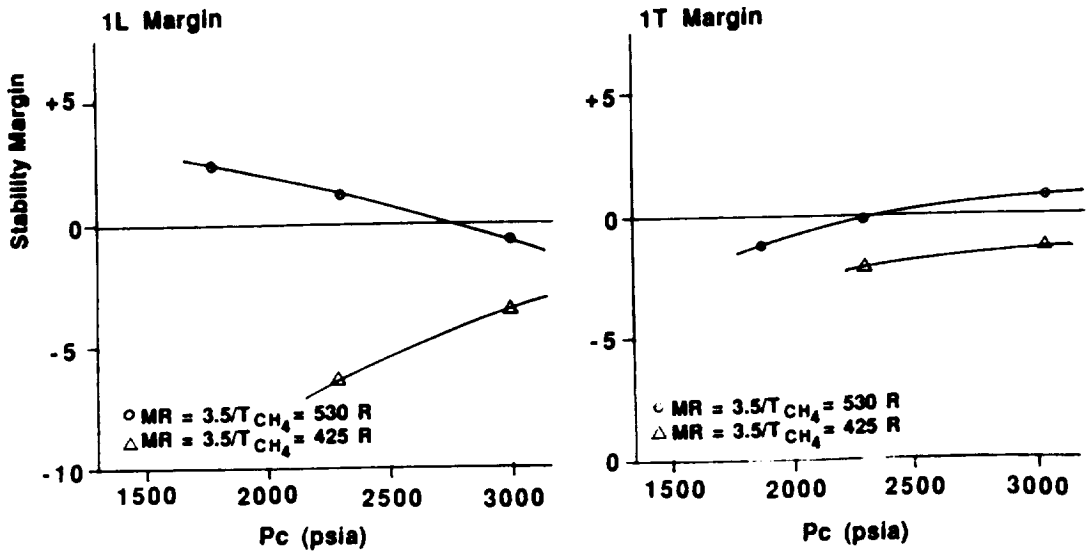

Figure 15. Stability Margin as a Function of Chamber Pressure for O/F = 3.5

increasing chamber pressure, was noted for the low mixture ratio operation, except for the 1L stability with ambient fuel. At this mixture ratio, fuel circuit stiffness is reduced from the low mixture ratio case. As the chamber pressure increases, the injector stiffness increases and time timelags decrease. In the case of the 1L, the methane timelag is nearly the same as the chamber's 1L timelag, and as chamber pressure increases, the oxygen timelag approaches this value faster than the fuel circuit stiffness increases.

CONCLUSIONS

Performance for the NASA/MSFC swirl coaxial injector should remain high at high chamber pressure and low fuel temperature. Compatibility should not be significantly influenced by planned test conditions. Stability margin is predicted to improve for ambient fuel temperature at higher chamber pressure but decrease with lower fuel temperature.

ACKNOWLEDGEMENT

Aerojet would like to thank C.R.Bailey and J. Hamilton of the Marshall Space Flight Center for their cooperation and assistance.

REFERENCES

1) Bailey, C.R. "Test Evaluation of Oxygen-Methane Main Injectors "1987 JANNAF Propulsion Meeting, December 1987.

2) Valler, H.W. "Design,Fabrication and Delivery of a High Pressure LOX-Methane Injector" Final Report Contract NAS8-33205 Report 33205F, Aerojet Liquid RocketCompany. November1979

3) Rupe, J.M. "The Liquid Phase Mixing of a Pair of ImpingingStreams", Progress Report 20-195 ORDCIP, Project Contract No. D9 04-495-ORO-18 August 1953.